Haptic-guided needle grasping in minimally invasive robotic surgery

Mario Selvaggio[1], Amir M. Ghalamzan E.[2], Rocco Moccia[1], Fanny Ficuciello[1] and Bruno Siciliano[1]

***Abstract*— In this work, we present preliminary results of a haptic-guided shared-control teleoperation system which aims to avoid encountering kinematic constraints on the da Vinci Research kit (dVRK). The main goal of such system is to *guide* the surgeon towards needle grasping configurations that are optimal, in the sense that they minimize the possibility of encountering joint limits and singularities along a suturing trajectory. To achieve this goal, we developed (*i*) a needle grasping parametrization and (*ii*) a gradient descent optimization method that minimizes the singularity and joint limits cost on the parametrized grasping manifold. Force cues are displayed through the dVRK master robot to guide the surgeon during the reach-to-grasp phase.**

I. Introduction

Autonomous robots are not yet sufficiently trusted in the surgical scenario because of safety-critical and high-consequence procedures they have to carry out. Remotely teleoperated surgical robotic systems represent the currently employed alternative solution. While they bring some advantages with respect to open procedures (such as tremor filtering and motion scaling), the robotic structure also imposes some constraints that restrict the surgeon movements. This additionally increases the human operator cognitive workload and causes severe fatigue and degeneration in performance.

Joint limits and singularities are common issues in master/slave manipulators. For example, they cause the surgeon to re-grasp the needle in the middle of suturing with hand-off movements [1]. This paper proposes a haptic shared control system for the da Vinci Research Kit (dVRK) that guides the surgeon in order to avoid such problems along suturing tasks. The proposed approach guides the operator during the reach-to-grasp phase towards a needle grasping configuration that results in neither joint limits nor singularities in the course of suturing.

II. Methods

In order to perform a suturing task which does not involve hands-off movements, we guide the surgeon towards a needle grasping configuration which yields no constraints during the stitching trajectory. We adopt a parametrization of needle grasping poses (Sect. II-A) and propose both a cost function and the corresponding optimization method to avoid joint limits and singularities (Sect. II-B). Our proposed solution inherently considers feasible grasping poses thanks to the projection of the cost function gradient on the space of feasible grasps. Then we use haptic guidance (Sect. II-C) to display optimal grasping configurations to the surgeon.

[1] Dipartimento Ingegneria Elettrica e Tecnologie dell'Informazione, Università di Napoli Federico II, Italy.
[2] School of Computer Science, University of Lincoln, UK.

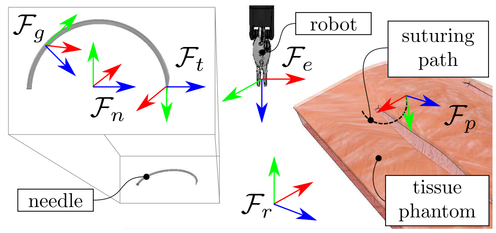

Fig. 1. Main reference frames and needle tip path (dashed black curve) for a single-stitch suturing task.

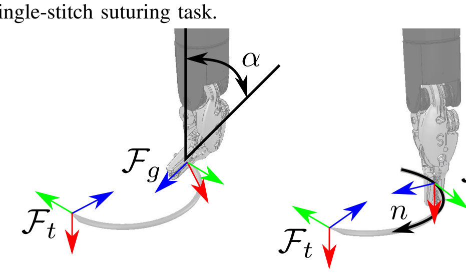

Fig. 2. Grasp parameterization by α (angle around the needle tangent) and n (needle curvilinear abscissa) [2], [3].

A. Needle parametrization

The subspace of possible grasping configurations can be conveniently parametrized by the needle curvilinear abscissa n and the angle around the needle tangent α (see Figs. 1-2). We denote by $\boldsymbol{z} = [n, \alpha]^T$ the vector identifying any point in the considered subspace $\mathcal{Z} \subseteq \mathbb{R}^2$. Hence, we can explicitly express $\mathcal{F}_e$ by $\boldsymbol{z}$, as ${}^r\boldsymbol{T}_e = {}^r\boldsymbol{T}_n{}^n\boldsymbol{T}_g$, ${}^n\boldsymbol{T}_g = \boldsymbol{T}_p(n)\boldsymbol{T}_r(\alpha)$. Considering $\dot{\boldsymbol{x}}_e = [\dot{\boldsymbol{p}}^T, \boldsymbol{\omega}^T]^T$ as the stacked vector of the Patient Side Manipulator (PSM) linear and angular velocities, the following equation holds

$$ {}^r\dot{\boldsymbol{x}}_e = {}^r\bar{\boldsymbol{R}}_n{}^n\dot{\boldsymbol{x}}_g = {}^r\bar{\boldsymbol{R}}_n\boldsymbol{J}_g\left(\boldsymbol{z}\right)\dot{\boldsymbol{z}}, \tag{1} $$

where ${}^r\bar{\boldsymbol{R}}_n \in \mathbb{R}^{6\times 6}$ transforms the twist coordinates from $\mathcal{F}_n$ onto $\mathcal{F}_r$ and $\boldsymbol{J}_g\left(\boldsymbol{z}\right) \in \mathbb{R}^{6\times 2}$ is the *grasp Jacobian* specific to the object shape and the choice of grasping parameters.

Combining the standard forward differential kinematics of the PSM, *i.e.* ${}^r\dot{\boldsymbol{x}}_e = \boldsymbol{J}_s(\boldsymbol{q}_s)\dot{\boldsymbol{q}}_s$ (where $\boldsymbol{J}_s$ is the conventional PSM geometric Jacobian) and (1) yields

$$ \dot{\boldsymbol{q}}_s = \boldsymbol{J}_s^{\dagger}(\boldsymbol{q}_s){}^r\bar{\boldsymbol{R}}_n\boldsymbol{J}_g\left(\boldsymbol{z}\right)\dot{\boldsymbol{z}}, \tag{2} $$

where $\boldsymbol{J}_s^{\dagger}$ denotes the usual Moore-Penrose pseudoinverse of the Jacobian matrix. Equations (1) and (2) are exploited in the following section to optimize the needle grasping pose using the gradient descent method.

B. Optimal grasping pose selection

To avoid constraints during post-grasp movements (*i.e.* the stitching trajectory), we define the following cost functions accounting for joint limits and Task-oriented Velocity (ToV) manipulability

$$h_j\left(\hat{\boldsymbol{q}}_g(t)\right) = \sum_{i=1}^{n} \frac{1}{\lambda} \frac{\left(\hat{q}_{g,i}^{+} - \hat{q}_{g,i}^{-}\right)^2}{\left(\hat{q}_{g,i}^{+} - \hat{q}_{g,i}(t)\right)\left(\hat{q}_{g,i}(t) - \hat{q}_{g,i}^{-}\right)}, \tag{3}$$

$$h_s\left(\hat{\boldsymbol{q}}_g(t)\right) = \dot{\hat{x}}^T(\boldsymbol{J}_s(\hat{\boldsymbol{q}}_g(t))\boldsymbol{J}_s(\hat{\boldsymbol{q}}_g(t))^T)^{-1}\dot{\hat{x}}, \tag{4}$$

where $\hat{\boldsymbol{q}}_g$ denotes the PSM joint values, $\lambda \in \mathbb{R}^+$ is a scalar constant, $\hat{q}_{g,i}(t)$ is the i^{th} joint coordinate at time t, $\hat{q}_{g,i}^{+}$ and $\hat{q}_{g,i}^{-}$ are its corresponding upper and lower limits, respectively, and $\dot{\hat{x}} = \dot{\boldsymbol{x}}/||\dot{\boldsymbol{x}}||$ denotes the velocity direction along which the manipulability is measured. Thus, the total cost is $h\left(\hat{\boldsymbol{q}}_g\right) = h_j\left(\hat{\boldsymbol{q}}_g\right) + h_s\left(\hat{\boldsymbol{q}}_g\right)$.

With s we parametrize a 6D single stitch suturing trajectory for the needle tip reference frame $\mathcal{F}_t$. Given the desired trajectory ${}^{r}\boldsymbol{T}_n(s)$, we can express $\hat{\boldsymbol{q}}_g$ as a function of s and $\boldsymbol{z}$. Thus, we can evaluate the cost along the trajectory as follows

$$\mathcal{H}\left(\boldsymbol{z}\right) = \int_0^{s^\star} h\left(\hat{\boldsymbol{q}}_g\left(s, {}^{r}\boldsymbol{T}_g\right)\right) \mathrm{d}s = \int_0^{s^\star} h\left(\hat{\boldsymbol{q}}_g\left(s, \boldsymbol{z}\right)\right) \mathrm{d}s. \tag{5}$$

We are looking for a parameters vector $\boldsymbol{z}$ that minimizes the cost function in (5). Mathematically, the problem writes as follows

$$\begin{aligned} \underset{\boldsymbol{z}}{\text{minimize}} \quad & \mathcal{H}\left(\hat{\boldsymbol{q}}_g\left(\boldsymbol{z}\right)\right) \\ \text{subject to} \quad & \boldsymbol{z}^{-} \le \boldsymbol{z} \le \boldsymbol{z}^{+} \end{aligned}. \tag{6}$$

The problem in (6) can be solved through the gradient descent iterative method. Each optimization step requires the update of $\boldsymbol{z}$ as $\boldsymbol{z}_{n+1} = \boldsymbol{z}_n - \gamma\nabla_{\boldsymbol{z}}\mathcal{H}$, where $\gamma \in \mathbb{R}^+$ represents the step increment and $\nabla_{\boldsymbol{z}}\mathcal{H}$ is the cost function gradient with respect to $\boldsymbol{z}$. Exploiting Leibniz's formula and the chain rule, the computation of $\nabla_{\boldsymbol{z}}\mathcal{H}$ writes as

$$\nabla_{\boldsymbol{z}}\mathcal{H} = \frac{\partial \mathcal{H}}{\partial \boldsymbol{z}} = \int_0^{s^\star} \frac{\partial h}{\partial \boldsymbol{z}} \mathrm{d}s, \qquad \frac{\partial h}{\partial \boldsymbol{z}} = \frac{\partial h}{\partial \boldsymbol{q}_s}\frac{\partial \boldsymbol{q}_s}{\partial \boldsymbol{z}}. \tag{7}$$

The term $\partial \boldsymbol{q}_s/\partial \boldsymbol{z}$ can be computed from (2) while the term $\partial h/\partial \boldsymbol{q}_s$ can be derived analytically from (5). Using (2) we can write the following relations

$$\frac{\partial \boldsymbol{q}_s}{\partial \boldsymbol{z}} = \boldsymbol{J}_s^{\dagger}(\boldsymbol{q}_s)^{r}\bar{\boldsymbol{R}}_n\boldsymbol{J}_g\left(\boldsymbol{z}\right), \quad \frac{\partial h}{\partial \boldsymbol{z}} = \frac{\partial h}{\partial \boldsymbol{q}_s}\boldsymbol{J}_s^{\dagger}(\boldsymbol{q}_s)^{r}\bar{\boldsymbol{R}}_n\boldsymbol{J}_g\left(\boldsymbol{z}\right). \tag{8}$$

At this point, it is easy to evaluate (7), thus finding the optimal grasping parameter vector $\boldsymbol{z}^{*}$. The optimal PSM Cartesian pose $\boldsymbol{x}_{g,d}$ can be calculated from the optimal grasping parameter vector $\boldsymbol{z}^{*}$ given the needle kinematics and its global pose.

C. Haptic Guidance

The purpose of haptic guidance is to guide the user toward the optimal grasping pose. Let $\boldsymbol{x}_{g,d} = [\boldsymbol{p}_{g,d}^{\mathrm{T}}, \boldsymbol{\phi}_{g,d}^{\mathrm{T}}]^{\mathrm{T}} \in \mathbb{R}^6$ be the optimal desired pose for the PSM end-effector frame $\mathcal{F}_e$, calculated by solving the optimization problem in (6), where $\boldsymbol{p}_{g,d} \in \mathbb{R}^3$ denote the position and $\boldsymbol{\phi}_{g,d} \in \mathbb{R}^3$ any parametrization of the orientation, *e.g.* Euler angles. The corresponding Master Tool Manipulator (MTM) desired pose $\boldsymbol{x}_{m,d} = [\boldsymbol{p}_{m,d}^{\mathrm{T}}, \boldsymbol{\phi}_{m,d}^{\mathrm{T}}]^{\mathrm{T}}$ can be calculated from $\boldsymbol{x}_{g,d}$ through the master-slave transformation $\boldsymbol{x}_{m,d} = \bar{\boldsymbol{R}}_c\boldsymbol{x}_{g,d} + \boldsymbol{x}_c$, where $\bar{\boldsymbol{R}}_c \in \mathbb{R}^{6\times 6}$ is the master-slave coupling rotation matrix and $\boldsymbol{x}_c = [\boldsymbol{p}_c^{\mathrm{T}}, \boldsymbol{\phi}_c^{\mathrm{T}}]^{\mathrm{T}} \in \mathbb{R}^6$ its offset. Given $\boldsymbol{x}_{m,d}$ we can display haptic cues on the MTM through impedance control.

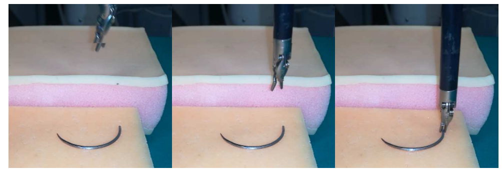

(a) Initial pose (b) Approaching (c) Grasping

Fig. 3. Snapshots from the optimal needle grasping experiment.

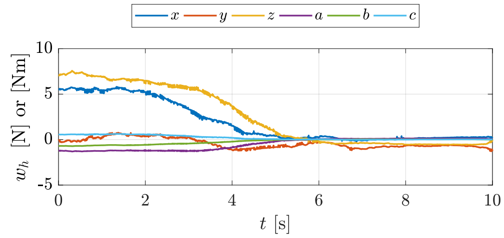

Fig. 4. Force guidance rendered by the Master Tool Manipulator during the haptic-guided needle grasping experiment.

D. Results

In our experiments, we considered a semi-circular stitching trajectory and obtained $\boldsymbol{x}_{g,d}$ by solving the problem (6) in Sect. II-B. This is used to generate force cues informing the human operator during the reach-to-grasp phase as discussed in Sect. II-C. Figure 3 shows snapshots from the experiments while the operator receives haptic cues shown in Fig. 4. The force intensity decreases by the closeness to the optimal grasping pose. Correspondingly, post-grasp movements during the suturing task execution are free from both joint limits and singularities.

III. Conclusions

In this paper, we presented preliminary results of a haptic-guided needle grasping method using the dVRK. Our approach minimizes the possibility of encountering joint limits and singularities along post-grasp suturing trajectory and inherently accounts for feasible grasping poses. The optimal grasp configuration is used to compute force cues which guide the operator's hand via the MTM. We illustrated the effectiveness of our proposed needle grasping approach using experiments performed on the dVRK.

References

[1] G. A. Fontanelli, M. Selvaggio, L. R. Buonocore, F. Ficuciello, L. Villani, and B. Siciliano, "A new laparoscopic tool with in-hand rolling capabilities for needle reorientation," *IEEE Robotics and Automation Letters*, vol. 3, no. 3, pp. 2354–2361, July 2018.

[2] F. Nageotte, P. Zanne, C. Doignon, and M. de Mathelin, "Stitching planning in laparoscopic surgery: Towards robot-assisted suturing," *The International Journal of Robotics Research*, vol. 28, no. 10, pp. 1303–1321, 2009.

[3] T. Liu and M. C. Cavusoglu, "Needle grasp and entry port selection for automatic execution of suturing tasks in robotic minimally invasive surgery," *IEEE Transactions on Automation Science and Engineering*, vol. 13, no. 2, pp. 552–563, 2016.